PHYSICAL REVIEW B **73**, 081401(R) (2006)

First-principles study of work functions of double-wall carbon nanotubes

Bin Shan
Department of Applied Physics, Stanford University, Stanford, California 94305-4040, USA

Kyeongjae Cho*
Department of Mechanical Engineering, Stanford University, Stanford, California 94305-4040, USA

(Received 27 November 2005; revised manuscript received 11 January 2006; published 6 February 2006)

Using first-principles density functional calculations, we investigated work functions (WFs) of thin double-walled nanotubes (DWNTs) with outertube diameters ranging from 1 to 1.5 nm. The results indicate that a work function change within this diameter range can be up to 0.5 eV, even for DWNTs with the same outer diameter. This is in contrast with single-walled nanotubes, which show negligible WF changes for diameters larger than 1 nm. We explain the WF change and the related charge redistribution in DWNTs using the charge equilibration model. The predicted work function variation of DWNTs indicates a potential difficulty in their nanoelectronic device applications.

DOI: 10.1103/PhysRevB.73.081401 PACS number(s): 31.15.Ar, 72.80.Rj, 73.30.+y

Double-walled nanotubes (DWNTs) have attracted considerable attention due to their electronic and mechanical properties.[1] Compared to single-walled nanotubes (SWNTs), they have higher mechanical stiffness and greater thermal stability, which may be of benefit in field emission devices.[2] Their double-shell structure offers the possibility of shielding the inner tube from external perturbations.[3] Such advantages make them very interesting for certain device applications.

The utilization of DWNTs in earlier days was largely hindered by the unwanted carbon nanomaterials generated at the same time with DWNTs during fabrication processes. Over the past few years, substantial improvements have been achieved in fabrication and purification techniques of DWNTs. Synthesis of high-quality DWNTs in a large scale has been realized using the high-temperature pulsed arc discharge technique[4] and the catalytic chemical vapor deposition.[5] In a more recent experiment, the production of DWNTs with the experiment yields more than 95% of what has been reported.[6] Thin DWNTs have also been successfully fabricated by filling C_{60} molecules in SWNTs followed by electron beam irradiation, yielding DWNTs with diameter distribution around 13–14Å.[7] In addition, it has now become possible to identify atomic correlations between adjacent graphene layers using high-resolution transmission electron microscopy,[8] enabling an unambiguous classification of DWNTs. All these point toward a possible application of DWNTs in nanoelectronic devices.

Recently, the potential use of DWNTs as channel materials for field-effect transistors (FETs) has been successfully demonstrated,[9] with better subthreshold swing factors as compared to SWNTs. Also, due to different inner and/or outer tube combinations and interlayer interactions, DWNTs-based FET yields richer transistor characteristics.[10] For a further large-scale integration of DWNT-based FETs, an understanding of the DWNT work function is essential, since even work functions that change on the order of 0.1 eV may lead to substantial changes in device characteristics.[11]

The encapsulation of molecules such as C_{60} inside SWNTs are known to modify the electronic properties of carbon nanotubes.[12] Due to their concentric double layer structures, ultrasmall diameter tubes can be encapsulated as the inner shell of DWNTs.[13] Nanotubes with diameters ~4 Å have already been observed in confined channels or as the inner shell of multiwall nanotubes.[14–16] The inner tubes in thin DWNTs usually feature high surface curvature and are shown to have large variations in work functions.[17] There have been some previous theoretical investigations on charge redistribution in selected DWNTs.[13,18] However, as far as we know, there has been no systematic study of the work functions of DWNTs and it remains unclear how the encapsulation of ultrasmall inner tubes affects the work functions of DWNTs.

In this study, we report first-principles work function calculations for two series of DWNTs consisting of either $(m,n)@(n,n)$ pairs or $(m,0)@(n,0)$ pairs $(m<n)$, with the first chiral index representing the inner tube and the latter representing the outer tube. The diameters of the DWNTs we studied range from 1 to 1.5 nm, within which work function variations are most significant. It was found that the work function variations can be up to 0.5 eV, even for DWNTs with similar outer diameters. This can be a significant value in device physics. The origin of work function modulations in DWNTs, as well as the charge redistribution, are shown to be correlated with the type of the inner shell, and can be qualitatively understood within the framework of the charge equilibration model (CEM). Some issues in the characterization and measurements of thin DWNTs are also discussed.

The work function was calculated using the standard procedure by taking the difference between the vacuum level ϕ and the Fermi level E_f. The vacuum level ϕ is determined from the average potential at the center of the vacuum region where it approaches a constant. We have excluded the slowly decaying exchange-correlation part of the potential in the vacuum region to achieve better convergence.[19] E_f was placed at the midgap in the case of a semiconducting DWNT. The calculation was done using the Vienna ab-initio simulation package[20] within the local density approximation (LDA). 30 k points were used along the nanotube's one-dimensional Brillouin zone, which was tested to give good convergence. In all simulations, an orthorhombic unit cell with cross-sectional dimensions of (35×35) Å^2 was used. With this unit cell size, the minimum separation between

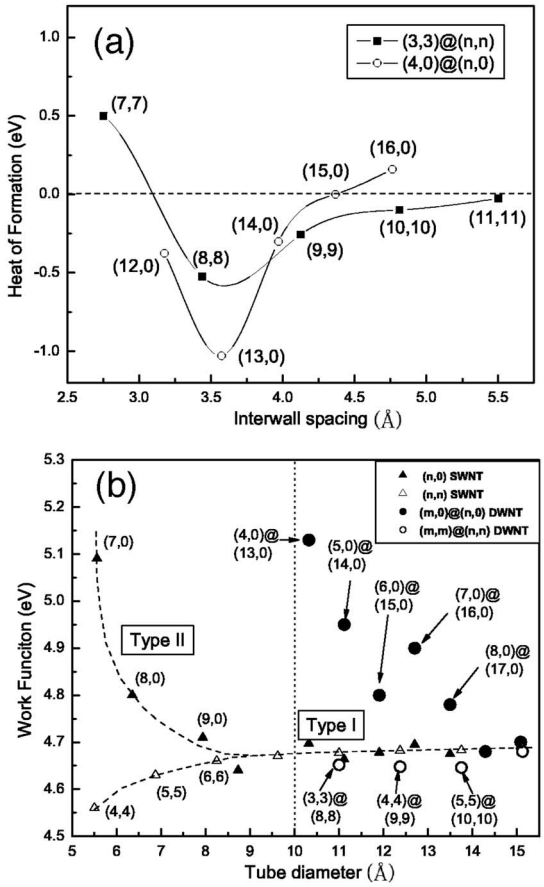

FIG. 1. (a) Heat of formation per unit cell for the DWNTs; solid square for (3,3)@(n,n) DWNTs and empty circle for (4,0)@(n,0) DWNTS. (b) Work functions for DWNTs (dots) and SWNTs (triangles) of different diameters.

periodic tube images was >18 Å, which ensures that the corresponding work function converges to a constant value. Kohn-Sham single-electron wave functions were expanded by 285 768 plane waves with an energy cutoff of 286.6 eV. For the LDA exchange-correlation potential, we have used a functional form fitted to the Monte Carlo results of homogeneous electron gas.[21] A conjugate-gradient method was used for both the electronic structure calculation and geometry optimization. The DWNTs were assumed to be fully relaxed when the force on each atom was less than 0.05 eV/Å.

We first discuss the stability and optimal interwall spacing for DWNTs. The energetics with respect to interwall spacing was calculated by fixing the innertube diameter and varying the diameter of the outer tube. Figure 1(a) shows the heat of formation for selected DWNTs $[\Delta E = E(DWNT) - E(SWNT)_{outer} - E(SWNT)_{inner}]$ with different interwall spacing. It was found that the most energetically favorable outer tube for (3,3) and (4,0) tubes are (8,8) and (13,0) tubes, respectively. For the two series of DWNTs we studied within the diameter range, the most stable inner-outer combination is consistently $(m,m)@(m+5,m+5)$ for armchair pairs and $(m,0)@(m+9,0)$ for zigzag pairs. The optimal interwall spacings corresponding to such combinations are close to the interlayer spacing of graphite (3.35 Å), possibly due to structural similarities between graphene sheets and nanotubes. This value of interwall spacing is consistent with other first-principles calculations[22] and experimental values from scanning tunneling microscope measurements.[23] Even though in real fabrication processes, DWNTs with nonoptimal interwall spacing are also expected to exist, those with optimal interwall spacing are more energetically favorable and would prevail in the final product. Moreover, similar correlation to the inner tube chirality was seen in DWNTs with nonoptimal interwall spacing. Thus, in the following, we will focus our discussion on work functions of DWNTs with optimal interwall spacing.

Figure 1(b) summarizes work functions of various DWNTs with optimal interwall spacing, plotted against the diameter of the outer tube. Also shown on the graph are work functions of SWNTs, indicated by the dotted line. As can be seen from the graph, there is essentially no diameter dependence of work functions for SWNTs larger than 1 nm (type-I SWNT). However, different work functions of DWNTs can be observed in the diameter range from 1 to 1.5 nm, for up to 0.5 eV. More specifically, $(m,0)@(n,0)$ DWNTs show a general decrease trend in work functions while those of $(m,m)@(n,n)$ pairs show little variation. This indicates that the work function difference is primarily due to the presence of the inner ultrasmall diameter tube (type-II SWNT), which is known to have substantial differences in work functions.[17] In particular, when the inner shell of the DWNTs is of $(m,0)$ zigzag type, the overall work function of the DWNT was increased due to the higher work functions of the inner tube.

The qualitative feature of the work function variations in DWNTs can be understood by the CEM, which has been successfully applied to molecular dynamics simulations.[24] Generally speaking, when two material systems with different chemical potentials (minus of work functions) come into contact, chemical potentials are equalized by electron transfer from a higher chemical potential system to a lower potential system. The total electrostatic energy of such a system can be written, neglecting higher order terms, as

$$E_{tot}(q_1,q_2,\cdots,q_N) = \sum_i^N \left[E_i^0 + \left(\frac{\partial E}{\partial q_i}\right) q_i + \frac{1}{2}\left(\frac{\partial^2 E}{\partial q_i^2}\right) q_i^2 \right] + \frac{1}{2}\sum_{i\neq j} V_{ij}(q_i,q_j) \quad (1)$$

$$= \sum_i^N \left(E_i^0 + \chi_i^0 q_i + \tfrac{1}{2} J_i^0 q_i^2\right) + \frac{1}{2}\sum_{i\neq j} V_{ij}(q_i,q_j), \quad (2)$$

where E_i^0 is the energy of neutral atom i, $-eq_i$ is the excess electrons on atom i, χ_i^0 is the electronegativity (minus of work functions), J_i^0 is the atomic hardness, and V_{ij} is the Coulombic interaction between atoms i and j. In the context of DWNTs, we can view the DWNT as a giant "molecule," with inner and outer tubes being two artificial "atoms" A and B. Taking the derivative of E_{tot} with respect to q_i, we arrive at the following equations for the chemical potential and charge transfer:

$$\chi_A(q) = \chi_A^0 + J_A^0 q + \frac{q}{2C}, \quad (3a)$$

TABLE I. Work functions of selected DWNTs.

DWNT	Tube diameter (Å)	Outer shell WF (eV)[a]	Inner shell WF (eV)[a]	WF from CEM (eV)	WF from DFT (eV)
(4,0)@(13,0)	10.32	4.70	5.95	5.32	5.13
(5,0)@(14,0)	11.11	4.66	5.10	4.88	5.00
(6,0)@(15,0)	11.91	4.68	4.99	4.84	4.80
(7,0)@(16,0)	12.70	4.69	5.10	4.90	4.90
(8,0)@(17,0)	13.49	4.69	4.80	4.74	4.77
(3,3)@(8,8)	11.00	4.68	4.50	4.59	4.64
(5,5)@(10,10)	13.75	4.68	4.63	4.66	4.64

[a]Work functions of SWNTs from Ref. 17

$$\chi_B(-q) = \chi_B^0 - J_B^0 q - \frac{q}{2C}, \tag{3b}$$

where $C=2\pi\varepsilon/\ln(b/a)$ is the unit length capacitance between two coaxial cylinders, with a and b being the inner- and outertube diameter, respectively. The dielectric constant of the nanotube is set to 1.[25] Under equilibrium, the electrochemical potential of the inner tube and outer tube must be equal. By equating $\chi_A(q)$ and $\chi_B(-q)$, we have the following first-order solution for the final chemical potential and charge transfer for DWNTs:

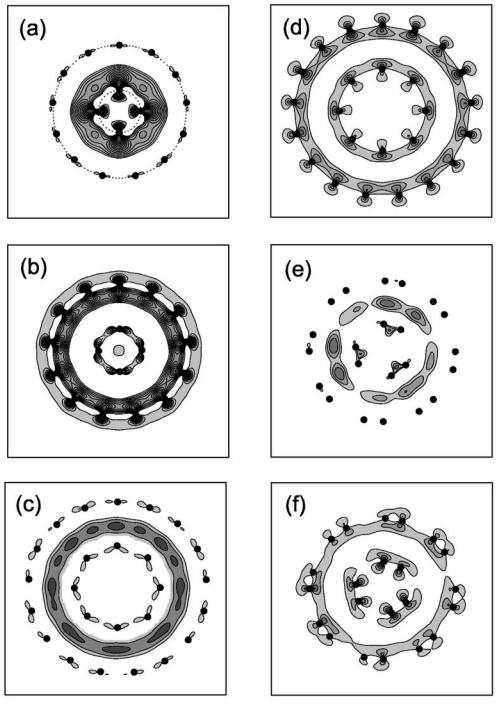

FIG. 2. Contour plots of charge accumulation (left column) and depletion region (right column) for (4,0)@(13,0), (8,0)@(17,0), and (3,3)@(8,8) DWNTs, respectivly. The contour plots are shown in a plane normal to the tube axis, with black dots indicating positions of carbon atoms. The contour value spacings are set to be equal.

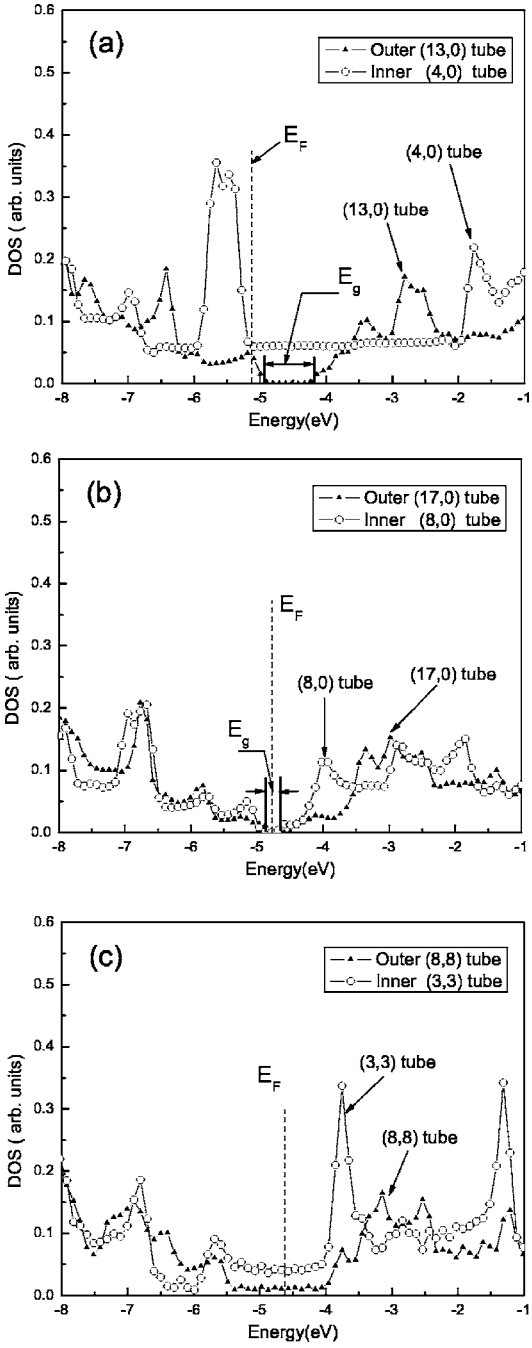

FIG. 3. Site-projected DOS for (4,0)@(13,0), (8,0)@(17,0), and (3,3)@(8,8) DWNTs, respectively. Empty circles for the outer tube and filled triangles for the inner tube.

$$q = \frac{\chi_B^0 - \chi_A^0}{J_A^0 + J_B^0 + 1/C}, \tag{4}$$

$$\chi = \frac{J_B^0 + \frac{1}{2C}}{J_A^0 + J_B^0 + \frac{1}{C}}\chi_A^0 + \frac{J_A^0 + \frac{1}{2C}}{J_A^0 + J_B^0 + \frac{1}{C}}\chi_B^0. \tag{5}$$

It can be seen that the direction and the amount of charge transfers are directly related to the work function difference between the inner and outer tubes, which is confirmed by

subsequent charge redistribution analysis. The final work function of the DWNT is a linear combination of work functions of the inner and outer tubes. Due to the small interlayer spacing and the resulting large $1/C$ term, the work function of the DWNT can be roughly approximated by the average of the work function of inner and outer tubes. Table I lists work functions predicted by the CEM as well as those from first-principles calculations. The general trend of the work function change predicted from CEM is in good agreement with the first-principles calculations, with the largest error $\sim$0.2 eV.

The charge redistribution in DWNTs is calculated by subtracting the charge distribution of isolated inner and outer tubes from the self-consistent charge distribution, $\Delta\rho = \rho(DWNT) - \rho(inner) - \rho(outer)$. Figures 2(a), 2(c), and 2(e) and Figs. 2(b), 2(d), and 2(f) show the charge accumulation regions and charge depletion regions, respectively. In (4,0)@(13,0) DWNT, the work function of the inner tube is $\sim$1 eV higher than that of the outer tube. Due to this large difference in work functions, the amount of charge transfers is also more significant than in other DWNTs, as indicated by the dense contour lines in Figs. 2(a) and 2(b). The direction of charge transfer can also be clearly identified. The accumulated charge mainly locates on the innertube (4,0) region rather in in the empty intertube region. Such charge transfer patterns have also been observed in (5,0)@(14,0) tubes. This indicates that provided a large enough work function difference, the direction of charge transfer can be predicted from SWNT work functions, consistent with one's physical intuition. In the case of (8,0)@(17,0) and (3,3)@(9,9) DWNTs, the work function difference of inner and outer tubes is not as large and the direction of charge transfer is more subtle due to the presence of interwall interaction. The depleted charge from the π electron system accumulates in the intertube region, with characteristics similar to the interlayer state in graphite systems. Such interlayer states in DWNTs have also been observed in other first-principles studies.[18] The amount of charge transfer is also smaller as evident by the sparse contour lines in Figs. 2(c)–2(f).

Finally, we discuss some possible issues in the characterization of thin DWNTs. Figure 3 shows the site-projected density of states (DOS), i.e., the local DOS integrated within spheres of the Wigner-Seitz radius centered on each ion, for the above three DWNTs. In $(m,0)@(n,0)$ DWNTs such as (4,0)@(13,0), the outer tube is semiconducting with low WF and the inner tube is metallic with high WF due to $\sigma-\pi$ hybridization.[26] When they form DWNT, substantial charge transfer from the outer tube to the inner tube leads to hole doping of the outer tube. Even though the band gap of the semiconducting outer tube is largely retained despite the interwall interaction, the Fermi level is below its valence band edge, giving rise to a finite DOS at the Fermi energy [Fig. 3(a)]. For those DWNTs with ultrasmall zigzag SWNTs as inner shells, their work functions are thus expected to be 0.2–0.5 eV higher than larger diameter DWNTs. As the DWNT diameter gets larger, such as for a (8,0)@(17,0) pair, the work functions of the inner and outer tube are comparable and their individual electronic structures are less perturbed. The DWNT is a semiconductor with a reduced band gap as compared to band gaps of both the outer and inner tubes [Fig. 3(b)]. (3,3)@(8,8) DWNT presents an interesting case. Even though it has almost the same diameter as (4,0)@(13,0) one and is also metallic, its electronic structure around the Fermi level is considerably different. Due to the presence of interwall interactions, states at the Fermi level are mostly localized in the inner tube with tails extending to the outer shell [Fig. 3(c)]. Its work function is about 0.5 eV lower than that of (4,0)@(13,0) DWNT, due to the higher WF of the inner tube.[17] These differences are likely to affect the transport and scanning tunneling microscope measurements of DWNTs.

In conclusion, we have systematically studied the work functions of the two series of DWNTs. It was found that the work function differences of DWNTs in a narrow diameter distribution (1.0–1.5 nm) can be up to 0.5 eV. The general trend of the work function change and charge redistribution are successfully explained by the CEM. These findings provide useful insight into the work function change in DWNTs that may be used to develop new ways of engineering electronic structures of DWNTs.

This work was supported by NSF grant on Network for Computational Nanotechnology (NCN). Part of the calculations were done at San Diego Supercomputing Center.

*Electronic address: kjcho@stanford.edu

[1] C. Wei *et al.*, Phys. Rev. B **67**, 115407 (2003).
[2] Y. W. Son *et al.*, Nanotechnology **16**, 125 (2005).
[3] M. Endo *et al.*, Nano Lett. **4**, 1451 (2004).
[4] T. Sugai *et al.*, Nano Lett. **3**, 769 (2003).
[5] E. Flahaut *et al.*, Chem. Commun. (Cambridge) **12**, 1442 (2003).
[6] M. Endo *et al.*, Nature **433**, 476 (2005).
[7] B. W. Smith *et al.*, Nature (London) **396**, 323 (1998).
[8] A. Hashimoto *et al.*, Phys. Rev. Lett. **94**, 045504 (2005).
[9] T. Shimada *et al.*, Appl. Phys. Lett. **84**, 2412 (2004).
[10] S. Wang *et al.*, J. Phys. Chem. B **109**, 17361 (2005).
[11] J. Guo and M. S. Lundstrom, IEEE Trans. Electron Devices **49**, 1897 (2002).
[12] Y. Cho *et al.*, Phys. Rev. Lett. **90**, 106402 (2003).
[13] Y. L. Mao *et al.*, Phys. Rev. B **71**, 033404 (2005).
[14] Z. M. Li *et al.*, Phys. Rev. Lett. **87**, 127401 (2001).
[15] L. C. Qin *et al.*, Nature **408**, 50 (2000).
[16] N. Wang *et al.*, Nature **408**, 51 (2000).
[17] B. Shan and K. Cho, Phys. Rev. Lett. **94**, 236602 (2005).
[18] Y. Miyamoto *et al.*, Phys. Rev. B **65**, 041402(R) (2002).
[19] T. C. Leung *et al.*, Phys. Rev. B **68**, 195408 (2003).
[20] G. Kresse and J. Furthmuller, Comput. Mater. Sci. **6**, 15 (1996).
[21] D. M. Ceperley and B. J. Alder, Phys. Rev. Lett. **45**, 566 (1980).
[22] J. C. Charlier and J. P. Michenaud, Phys. Rev. Lett. **70**, 1858 (1993).
[23] M. H. Ge and K. Sattler, Science **260**, 515 (1993).
[24] A. K. Rappe and W. A. Goddard, J. Phys. Chem. **95**, 3358 (1991).
[25] F. Leonard and J. Tersoff, Appl. Phys. Lett. **81**, 4835 (2002).
[26] X. Blase *et al.*, Phys. Rev. Lett. **72**, 1878 (1994).